

DJB 4/8/87



STUDIECENTRUM VOOR KERNENERGIE

C  
E  
N  
T  
R  
E  
  
D  
E  
T  
U  
D  
E  
  
D  
E  
  
L  
E  
N  
E  
R  
G  
I  
E  
  
N  
U  
C  
L  
E  
A  
I  
R  
E

For presentation at the

IAEA Co-ordinated Research Meeting

PERFORMANCE OF SOLIDIFIED HIGH-LEVEL WASTE FORMS AND  
ENGINEERED BARRIERS UNDER REPOSITORY CONDITIONS

SYDNEY, Australia, 6-10 April 1987

IN SITU TESTING OF NUCLEAR WASTE FORMS IN AN UNDERGROUND  
LABORATORY IN CLAY

P. VAN ISEGHEM, W. TIMMERMANS  
Materials Physics Department  
W. DEBRUYN, J. DRESSELAERS  
Metallurgy Department  
B. NEERDAEL  
Nuclear Chemistry Department

S.C.K./C.E.N., B-2400 MOL (Belgium)

8906120323 870423  
NMSS SUBJ  
412 CF

IN SITU TESTING OF NUCLEAR WASTE FORMS IN AN UNDERGROUND  
LABORATORY IN CLAY

P. VAN ISEGHEM\*, W. TIMMERMANS  
Materials Physics Department  
W. DEBRUYN, J. DRESSELAERS  
Metallurgy Department  
B. NEERDAEL  
Nuclear Chemistry Department  
S.C.K./C.E.N., B-2400 MOL (Belgium)

ABSTRACT

During 1986 a number of simulated waste forms (HLW and TRUW glasses and glass-ceramics) have been, or will be buried in the underground laboratory in clay in Mol. Their corrosion rate will be measured in two environments susceptible to contact the conditioned radioactive waste during its geological storage in a clay formation: host clay and a humid atmosphere loaded with clay extracts. The experiments, with total exposure times of 50.000 h, will be carried out at various temperatures: 15, 50, 90, 170°C.

This paper describes the experimental concept, the location in the laboratory and the various in-situ and post-corrosion analyses. It also focusses on a blank overcoring test, related with the retrieval of the corrosion tubes at the end of the test. Preliminary results are given on the settling of the host clay on the corrosion tubes, and on the in situ water permeability of the filter elements used for the clay atmosphere experiments.

INTRODUCTION

Over the past several years, S.C.K./C.E.N. has been pursuing an extensive research programme aimed at evaluating the suitability of a clay formation, situated under the nuclear site at Mol, as a host rock for storing conditioned nuclear waste. As part of this programme, an underground laboratory has been built (see Fig. 1) to gather the essential geomechanical informations required for the feasibility study of the concept [1]; in the

meantime, clay cores have been sampled for laboratory examination. The underground laboratory further provides small scale in-situ experiments to study heat transfer, migration of radionuclides, corrosion of candidate structure and container materials, and corrosion of candidate waste forms [2,3]. These experiments should enable validation of the results from similar experiments performed in laboratory conditions. They will also provide experience with various in situ measuring techniques.

To prove the feasibility and the performance assessment of storing high level and/or long living nuclear waste in clay, an extension of the present underground laboratory is being designed. This extension will be used for combined experiments - possibly including larger scale ones - and emphasize the aspect of radiation.

This paper describes the concept and status of implementation of the in situ corrosion tests on candidate waste forms. The experiments were conceived in such a way that they could be used at the same time for corrosion tests on metallic container and structural materials, and on simulated waste forms. One type of set-up is designed for investigating corrosion of the materials in contact with the geological clay formation - what is likely to occur at the disposal facility after long exposure times. A second set-up is aimed at studying the corrosiveness of the atmosphere issued from the clay formation. This atmosphere would contact the waste form container in case of failure of the gallery structure material in the course of, e.g., the first hundreds of years, through capillarities in the backfill between the gallery and the container. To simulate the thermal effect of the waste canisters, the experiments will be performed not only at the temperature of the clay body ( $\approx 15^{\circ}\text{C}$ ), but also at two or three higher temperatures.

#### 1. EXPERIMENTAL CONCEPT

The experimental design is to a large extent based on the experience gained in preliminary experiments, performed between 1979 and 1983 in a surface clay quarry (Terhagen, 50 km to the west of Mol), covering the same ("Boom") clay formation [4]. For both types of tests the set-up includes container material and waste form samples. Both set-ups were designed to provide the interaction with non disturbed (i.e. non frozen) clay. Non disturbed clay can be found at a distance of 4 m from the gallery wall [1].

Fig. 2 shows the design for the interaction tests in contact with the clay derived atmosphere. Four tubes have been manufactured, to perform separately tests at ambient temperature ( $\approx 15^{\circ}\text{C}$ ), 50, 90 (which is close to

100°C, the maximum temperature allowed for the clay repository) and 170°C (a reference, "safety" temperature selected within the European Community). The tubes are to be inserted vertically downwards in the clay formation and connected to the bolted cast iron wall of the experimental gallery. They end in a porous (pore size 5  $\mu\text{m}$ ), stainless steel plug. Helium carrier gas collects the corrosive products perspiring from the clay through the steel filter into the tube, and circulates these products over the test samples, placed inside the heating section.

The waste form samples (30x30x3mm) are mounted in a teflon boat, which is heated at the specified temperature using resistance heating. The teflon boat can be removed and exchanged during the experimental period. In addition to the continuous measurement of the temperature in the corrosion chamber, a number of analyses will be performed on the clay extracts (see Fig. 3). The dew point and pH will be measured on line periodically. The chemical composition will be determined on the condensed ( $- 80^\circ\text{C}$ ) extracts; alternatively, the chemical composition may be determined on line continuously, by infrared absorption. (Typical values measured in the surface quarry tests were, in  $\text{mg l}^{-1}$ : 50-20000 CO-CO<sub>2</sub>;  $\leq 800$  NO-NO<sub>2</sub>;  $\leq 100$  SO<sub>2</sub>;  $\leq 100$  HCl) [4].

Fig. 4 shows the design for the interaction tests involving direct contact with the clay host rock. Four tubes have been manufactured, enabling separate tests at clay temperature ( $\approx 15^\circ\text{C}$ ), 90 (two tubes, for two different interaction times) and 170°C. The tubes, with the waste form (40x15x5mm) and ring-shaped container samples ( $\phi \approx 10$  cm) fixed at the outside, are introduced horizontally into the clay body and connected to the experimental gallery. They are heated by a retractable furnace situated in their interior. The furnace consists of heating wires spirally wound around a stainless steel support tube.

During the experiments in both clay and clay extracts, the temperature and  $\text{pH-E}_h$  at the interface waste form/clay will be continuously monitored. The pH will be measured with commercially available high pressure resistant glass electrodes, encapsulated in a metallic housing to resist local, lithostatic pressures. The redox potential will be measured as shown in Fig. 5. The Pt and Au measuring electrodes are mounted on the outer wall of the corrosion tubes. A solid body type Ag/AgCl reference electrode is installed close to the measuring electrodes. This reference electrode is based on a KCl containing acrylic polymer. An additional set of electrodes is to be introduced, however, to detect and compensate for eventual parasitic potentials (due to the presence of a barrier of thermally non uniform clay between the main measuring and reference electrodes).

## 2. EXPERIMENTAL PROGRAMME

The clay contact tubes can incorporate 64 waste form samples. Both HLW and TRUW glass samples are considered:

- Simulated high level waste glasses:  
UK209, SON58, SON64, SON68, SAN60, SM58, SM513, BEL-15, SRL131/29.8 % TDS, SRL131/35 % TDS, SRL165/TDS [5-7];
- Incinerated alpha waste compacts: FLK77 [8];
- Alpha waste incinerator slag simulant glasses UWG119, 122, 123, 124 [8];
- Simulated waste glass-ceramics, resulting from isothermal annealing of the parent glasses:  
C31 [5], SAN60, SM58; UWG119, 122, 123, 124 [8].

All different waste forms are loaded in twofold.

Besides, some combined waste glass/metal container samples will be loaded too, to evaluate the influence of the presence of container corrosion products on the waste glass performance. Each of HLW glasses SON68, SM58, SAN60 and TRUW-FLK77 will be combined with each of the candidate container materials titanium, carbon steel and Hastelloy C4. Furthermore one of the 90°C tubes is loaded with a sample of SM513 and SON68, tracers with Pu, Cs and Sr (19MBq Pu-239, 22 MBq Sr-90, and 33 MBq Cs-134 per sample).

Three tubes will be retrieved after 50.000 h interaction time; one of the 90°C tubes will be retrieved after a 15.000 h residence. The tube retrieval will be performed by overcoring, i.e. including a clay layer of about 10 cm thick. One of each waste form samples will be used for the measurement of the mass loss and for surface analysis (e.g. SEM-EDXA), the second sample will be cross-sectioned, and analysed for its thickness, and elemental distribution in the surrounding clay, in the waste form surface layer and in the bulk (by, e.g. EMPA X-ray analysis and SIMS). Elemental analysis of the surrounding clay will be especially significant in the case of the tracers, since these tracers were selected on the basis of their wide range of diffusivity through clay (in  $\text{cm}^2\text{s}^{-1} = 2 \times 10^{-7}$  for Sr,  $1 \times 10^{-8}$  for Cs,  $1 \times 10^{-9}$  for Pu [9]).

About 20 waste form specimens will be loaded in each clay atmosphere tube. The following waste forms will be tested: HLW glasses SON68, SAN60, SM513 (amorphous or partially crystallized), HLW glass-ceramic C31, TRUW glasses FLK77, UWG124 (amorphous or partially crystallized). It is planned to retrieve the waste form boats after various corrosion times; the longest time might be 50.000 h. The post corrosion analyses on the waste form samples will be similar to the clay contact experiments.

### 3. STATUS OF IMPLEMENTATION

Before introduction of the experimental tubes, a blank test was performed for the retrieval of a corrosion tube together with some 10 cm thick clay layer (see: experimental programme). A 6 m long corrosion tube of 10 cm diameter, horizontally emplaced in the clay and completely caught as a result of the plastic deformation of the clay, has been recovered in several steps. First a 4 m long steel jacket, 75 cm in diameter was introduced concentrically with the corrosion tube. Internal material was blown out. Then a number of small ( $\phi$  12 cm) holes were drilled at the periphery to release the test section of the tube (where the waste form samples are mounted) together with surrounding clay (see Fig. 6). Hydraulic jackets were used to remove the tube/clay sample.

All clay contact tubes were installed by early 1986. Their position in the underground laboratory is given in Fig. 7. Their implantation was chosen in such a way that there will be no mutual thermal disturbance, even in the long term. The minimum distances between the various tubes were determined from model calculations [10] to be 1.2 m (170-90°C), 5 m (170-50°C) and 21 m (170-20°C). Presently the tubes are being slowly heated up. In this initial phase, there is still an important temperature gradient between the inner heating elements and the interface waste form/clay (90 versus 20°C, respectively), suggesting that the surrounding clay has settled, indeed. Another evidence of the settling of the clay is given by electrical conductivity measurements in the vicinity of the corrosion tube and on clay samples in laboratory. Both measurements yield values of about  $3 \times 10^{-5} \Omega^{-1} \text{m}^{-1}$ .

All four clay atmosphere interaction tubes are planned to be installed by mid 1986 (positions, see Fig. 7), allowing full operation of the experiments by the end of 1986. To test the permeability of the porous outer filter element in real conditions, one of them has been introduced at a depth of about 5 m below the gallery lining (end of 1985), without addition of the heating elements, ... A pore water flux of  $55 \text{ ml m}^{-2} \text{ d}^{-1}$  has been measured, which fits with the theoretically and experimentally derived clay permeability/pressure relationship, supposing the pore water pressure at the filter position is about 0.5 MPa.

### ACKNOWLEDGEMENTS

This work has been performed with partial financial support from the Commission of the European Communities and NIRAS/ONDRAF (the National Agency for Radio-active Waste and Fuel). Helpful discussions with Dr. R. De Batist and Dr. R. Leysen, and technical assistance from Messrs. J. Kelchtermans and M. Segers are gratefully acknowledged.

### REFERENCES

- <sup>1</sup>P. Manfroy, R. Heremans and A. Bonne, "Ten years of site specific research and its relevance to the concept of a waste disposal system in clay", presented at the International Meeting on High-Level Nuclear Waste Disposal Technology and Engineering, Pasco (USA), September (1985).
- <sup>2</sup>P. Manfroy, B. Neerdael and M. Buyens, "Expérience acquise à l'occasion de la réalisation d'une campagne géotechnique dans une argile profonde"; p. 248 in Design and Instrumentation of In Situ Experiments in Underground Laboratories for Radioactive Waste Disposal, Edited by B. Côme, P. Johnston and A. Müller, EUR 9575 (1985).
- <sup>3</sup>F. Casteels, J. Dresselaers, J. Kelchtermans, R. De Batist and W. Timmermans, "In situ testing and corrosion monitoring in a geological clay formation"; p. 277 in Design and Instrumentation of In Situ Experiments in Underground Laboratories for Radioactive Waste Disposal, Edited by B. Côme, P. Johnston and A. Müller, EUR 9575 (1985).
- <sup>4</sup>F. Casteels, H. Tas, R. Heremans and M. Brabers, "Corrosion of materials in a clay environment"; p. 944 in Chemistry and Process Engineering for High-Level Liquid Waste Solidification, Edited by R. Odoj and E. Merz, Jül-Conf-42 (vol. 2) (1981).
- <sup>5</sup>Testing and Evaluation of Solidified High-Level Waste Forms, Joint annual progress report 1983 to the CEC, Edited by G. Malow, EUR 10038 (1985).
- <sup>6</sup>G.G. Wicks, "WIPP/SRL in situ and laboratory testing programs - part I: MITT overview, non-radioactive waste glass studies", DP1706 (1985).
- <sup>7</sup>A. Donato, Ji-Fu Zhang, V. Gottardi, A. Soraru, "A borosilicate glass for the EUREX high level waste, characterization and behaviour", p. 327 in Radioactive Waste Products - Suitability for Final Disposal, Edited by E. Merz, R. Odoj and E. Warnecke, Jül-Conf-54 (1985).
- <sup>8</sup>P. Van Iseghem, W. Timmermans and R. De Batist, "The characterization of ceramic incinerator slags and their simulants", p. 27 in Testing, Evaluation and Shallow Land Burial of Low and Medium Radioactive Waste Forms, Edited by W. Krischer and R. Simon, EUR 8979 (1984).

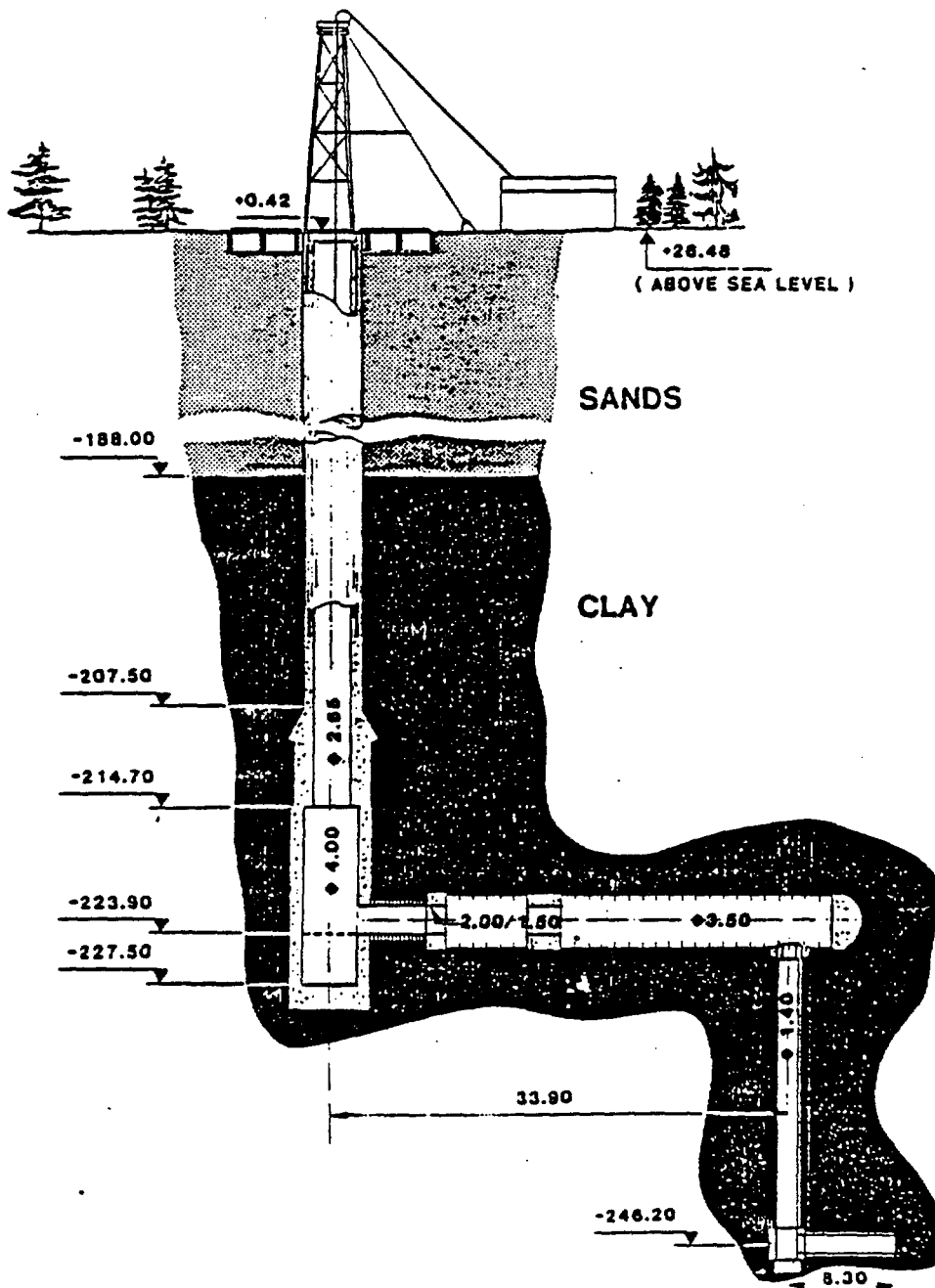
<sup>9</sup>P. Henrion, M. Monsecour and M. Put, "Migration studies of radionuclides in Boom clay", presented at the Symposium on Clay Barriers for Isolation of Toxic Chemical Waste, Stockholm (Sweden), May 1984.

<sup>10</sup>M. Put, private communication.

CAPTIONS FOR FIGURES

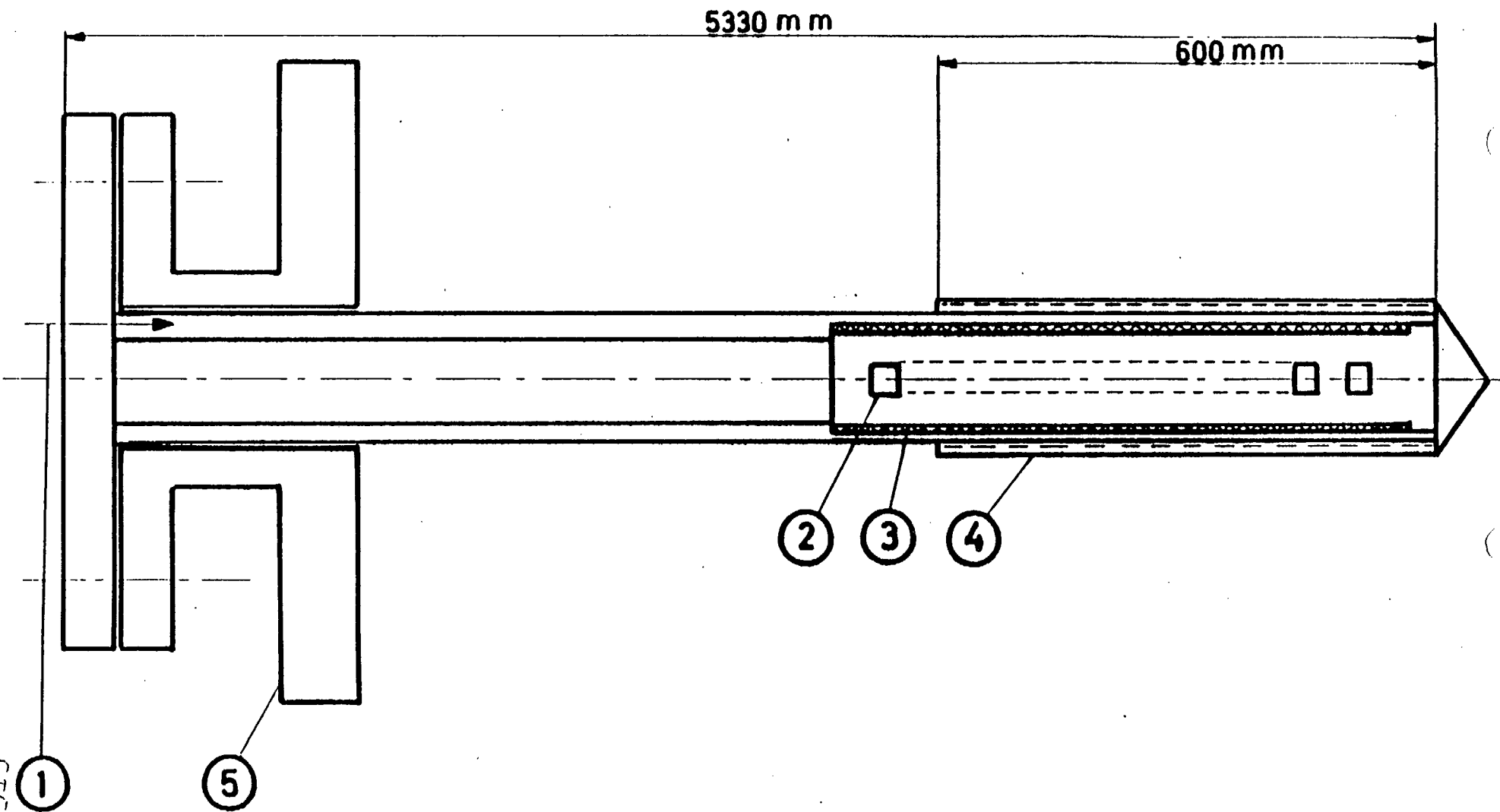
- FIG. 1. Scheme of the as built underground experimental facility.
- FIG. 2. Schematic view of the corrosion tube for the tests in contact with the clay derived atmosphere
1. Gas inlet
  2. Container and waste form samples
  3. Heating elements
  4. Porous filter
  5. Gallery.
- FIG. 3. Block diagram of the instrumentation for the corrosion experiments in clay atmosphere.
- FIG. 4. Schematic view of the corrosion tube for the tests in direct contact with clay
1. Gallery
  2. Container samples
  3. Waste form samples
  4. Heating elements.
- FIG. 5. Positions of the various pH and  $E_h$  electrodes.
- FIG. 6. Schematic view of the overcoring test, with:
- phase 1, the removal of a clay core, 4 m long, 0.75 m diameter
  - phase 2, the overcoring of the end section of the tube.
- FIG. 7. Positions of the different access holes in the gallery lining (unfolded)
- the clay contact tubes are loaded in holes A, B, D and M
  - the clay atmosphere tubes are loaded in holes 7, 13, 19 and 60.

GE/058/84

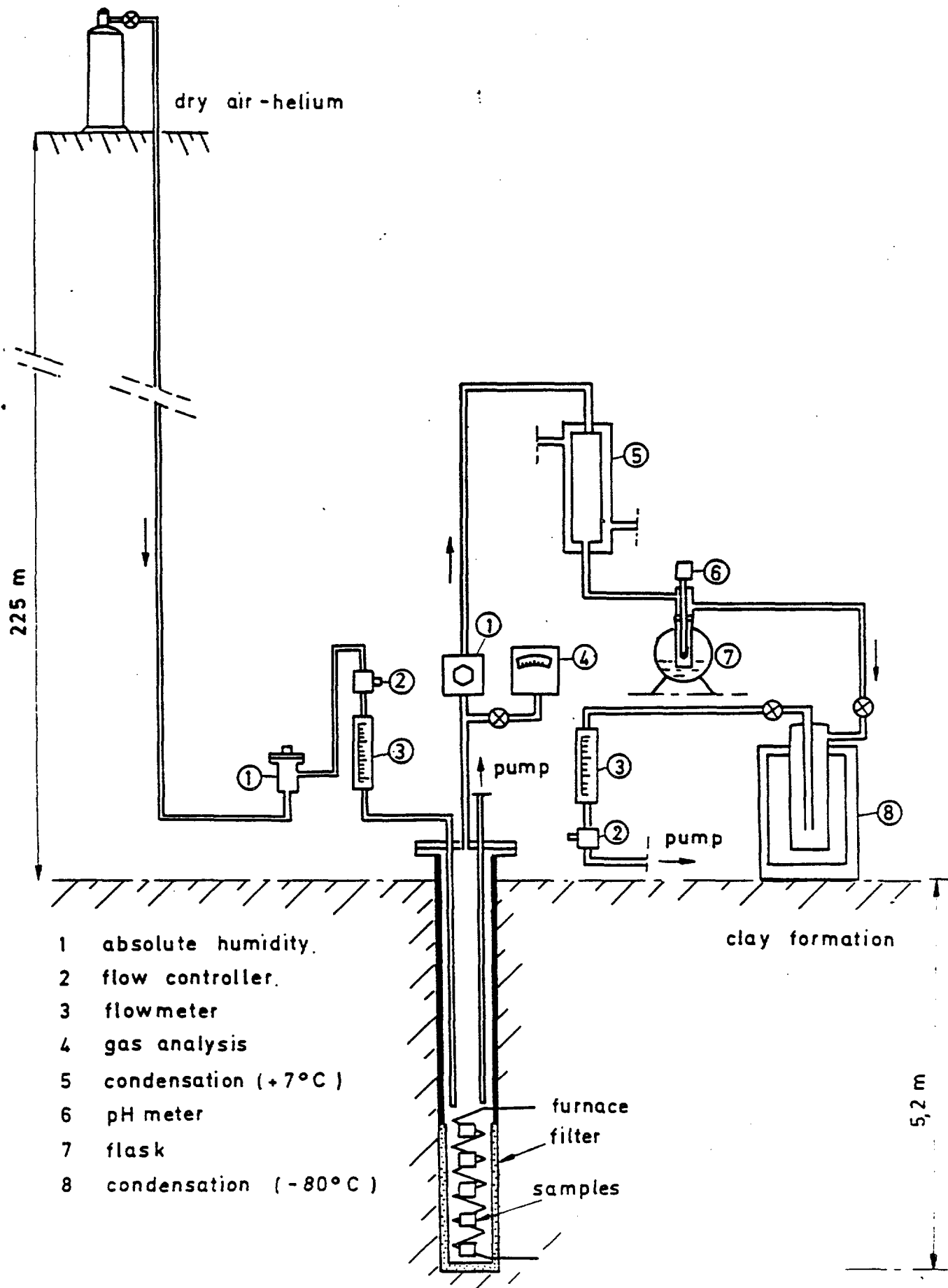


SCHEME OF THE AS BUILT  
UNDERGROUND EXPERIMENTAL FACILITY

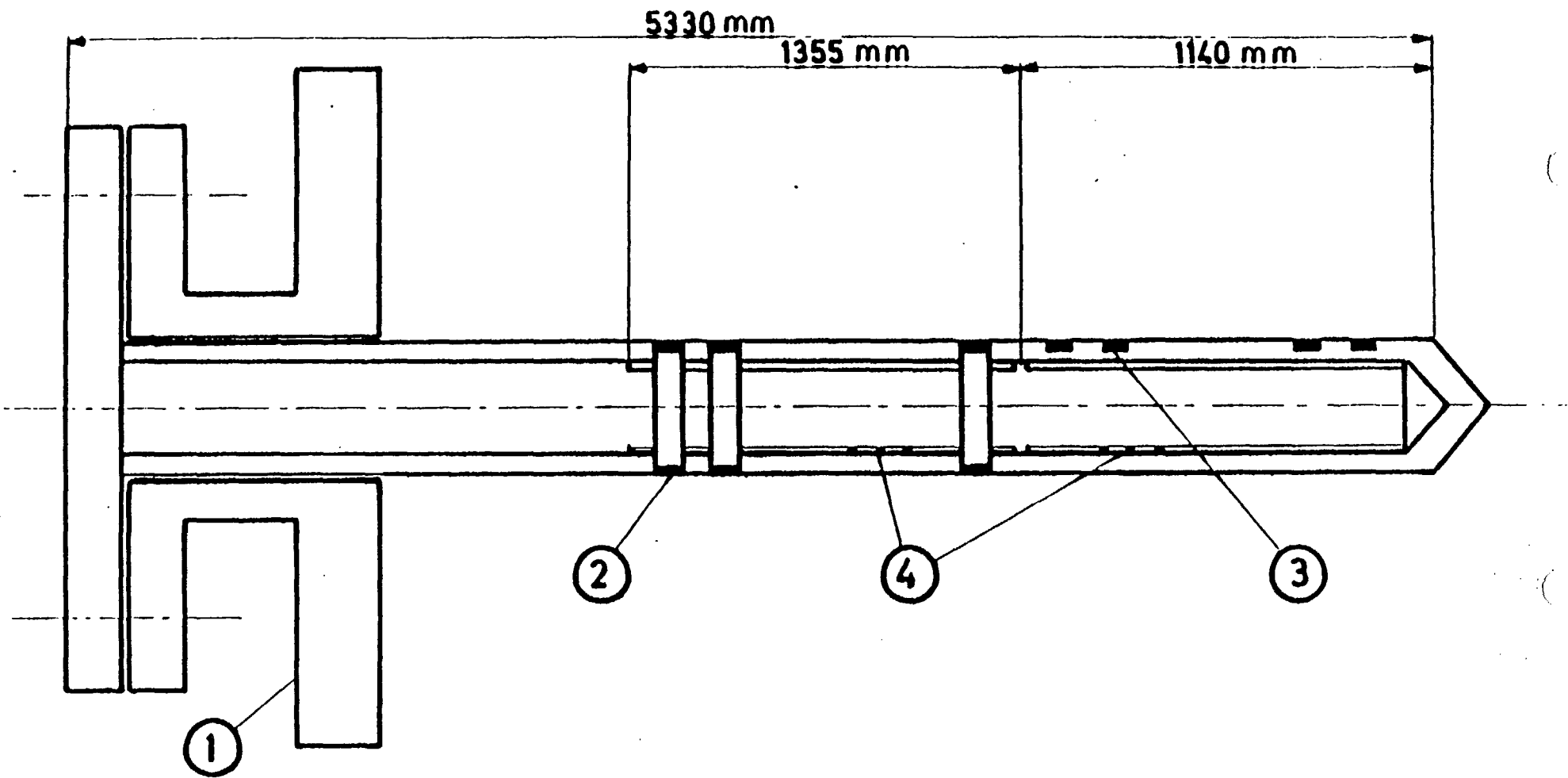
SCK/CEN



- FIG 2 -



- FIG 3 -



- FIG 4 -

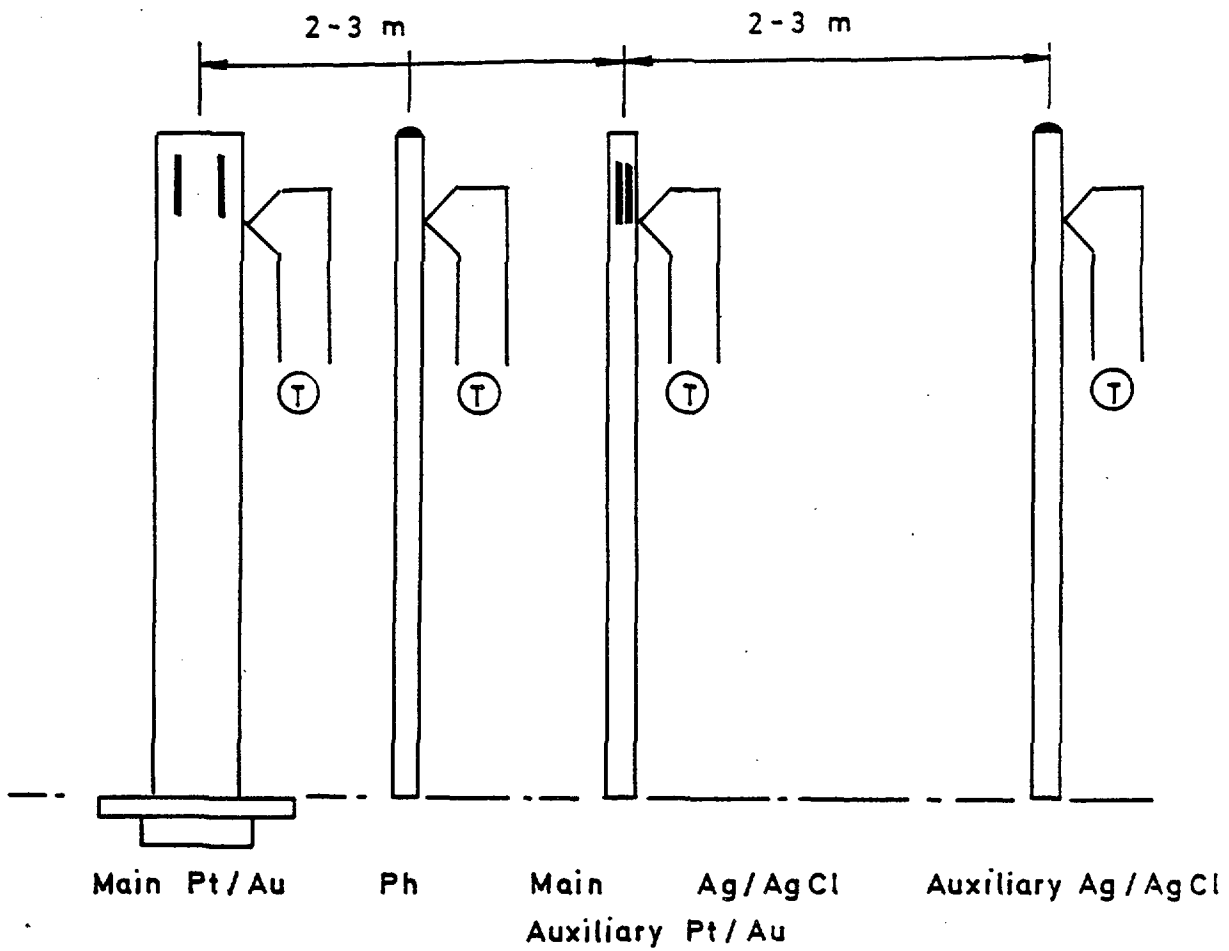
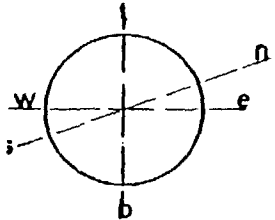
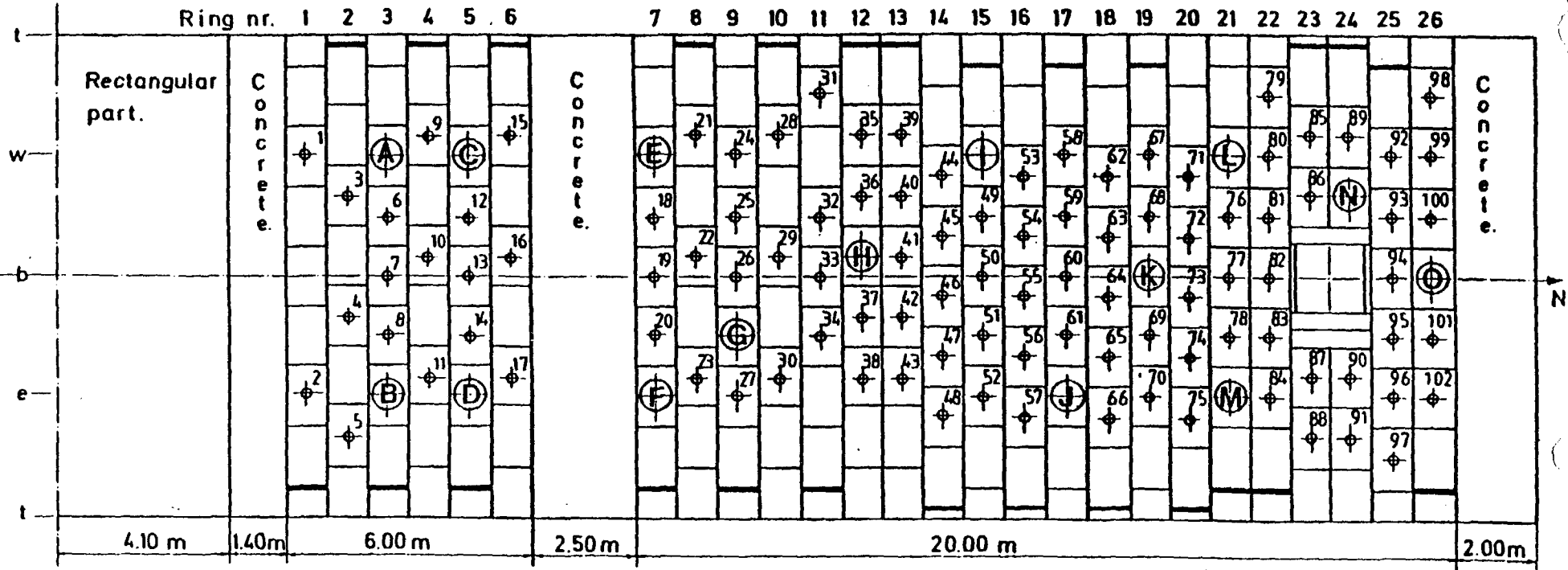
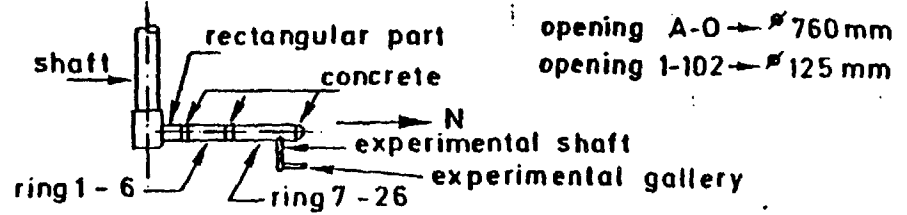


Fig.. Two dimensional view of the pH/Eh electrodes.



t = top  
b = bottom  
n = north  
e = east  
s = south  
w = west



POSITIONS OF THE DIFFERENT ACCESS HOLES  
IN THE GALLERY LINING (UNFOLDED)

FIG 2

SCK / CEN

DJB 4/7/87

Dr. Berthold LUCKSCHEITER  
Kernforschungszentrum Karlsruhe  
Institut für Nukleare Entsorgungstechnik  
Postfach 3640, D-7500 Karlsruhe 1  
Federal Republic of Germany

International Atomic Energy Agency

Second Research Coordination Meeting on  
The Performance of Solidified High-Level Waste Forms  
and Engineered Barriers Under Repository Conditions

Australian Atomic Energy Commission (AAEC)

Sydney, Australia, April 6-10, 1987

**TABLE OF CONTENTS**

- **ACTIVE PAMELA-OPERATION**
- **PROCESS CHEMISTRY OF HLLW-VITRIFICATION**
- **CHARACTERIZATION OF GLASS PRODUCTS FOR VITRIFICATION OF HLLW**
- **INVESTIGATION OF FULL-SCALE GLASS BLOCK CANISTERS**
- **FUTURE ACTIVITIES IN INE/KfK**

## Active PAMELA-Operation

### 1. Objectives of the PAMELA-vitrification plant

The PAMELA-plant in Mol/Belgium was constructed as a pilot plant to demonstrate

- the vitrification process,
- acceptability of glass products,
- environmental impact: release to stack,
- radiation exposure of personnel,
- quality assurance of final glass product.

The hot demonstration should supply all required design data for

- erection and operation licence for the PAMELA-WAW-plant,
- establishment of Waste Acceptance Criteria for final storage.

Further objectives are

- vitrification of 800 m<sup>3</sup> HEWC (High Enriched Waste Concentrate) in Mol,
- vitrification of 65 m<sup>3</sup> HAWC stored in the WAK-plant in Karlsruhe.

From October 1985 to June 1986 50 m<sup>3</sup> LEWC, stored in two tanks with about 100 Ci/m<sup>3</sup>  $\beta/\gamma$ -activity, were vitrified to 78 tonnes of waste glass, 440 glass blocks and 100 blocks of "Vitromet" have been produced.

### 2. Data of the PAMELA-operation

Details of the four LEWC-campaigns are given in Table 1.

The LEWC-glass should have a waste loading of 11 wt.%. This loading was attained in the 2nd and 3rd campaign when the LEWC of the 2nd storage tank was vitrified. The waste solution in the 1st tank had a lower salt-content but a higher Na-concentration. As the total Na<sub>2</sub>O-content in the waste glass should not exceed 9.5 wt.% (for viscosity reasons), the glass loading had to be reduced to 8.6 wt.%.

During the active vitrification runs, glass samples were taken regularly from the waste glass (Vitromet-beads or small pieces from the glass filament on the Inconel outlet tube). The glass samples were melted with  $K_2CO_3$ , dissolved in  $HNO_3$  and then analysed by ICP-measurement. Moreover, the Cs-137 activity was measured and compared with the Cs-137 activity in the LEWC-calciate. From the relation of these two activities the waste loading of the waste glass can be determined. The analysed elemental glass composition of samples from the campaign II and III corresponded with the calculated target composition given in Table 2.

The limiting factors for the waste loading is the presence of sulphur and the high concentration of sodium in the waste solution (Fig.1) by which a separate phase, so-called "yellow phase", is formed on top of the glass pool. This yellow phase is at room temperature a crystalline mixture of  $LiNaSO_4$ - $LiNaCrO_4$ ,  $CaMoO_4$  and  $Na_2SO_4$ .

Under steady state conditions and as long as the content of the LEWC-oxides in the glass melt is 11 wt.% or less, the separate phase is absorbed by the glass melt. Accumulation of the yellow phase can cause increased material loss into the off-gas system because of its high volatility.

The HAWC of the WAW (Fig.1) contains no sulphur but a relatively high amount of molybdenum. The solubility of Mo in the glass melt which controls the waste loading of the glass product is about 2%. In vitrification runs with HLLW-simulate Mo-rich yellow phase was frequently observed in the "cold cap" region of the glass pool surface and sometimes even inside the glass blocks. The composition of this phase is shown in Fig.2.

### 3. Vitrification of HEWC

The vitrification of the HEWC with the PAMELA-plant started in October 1986. For the vitrification of the 800 m<sup>3</sup> HEWC about four and a half years are necessary. In this time about 310 tonnes of glass in 800 canisters with 430 mm diameter and a glass volume of 150 l will be produced.

Compositions of calcined HEWC are given in Tab.3. The very high Al<sub>2</sub>O<sub>3</sub> content and the relatively high content of SO<sub>4</sub><sup>2-</sup> and HgO are remarkable. About 90% of the calcinate consists of Al<sub>2</sub>O<sub>3</sub>. The total β-activity is below 10 Ci/l.

To reduce the total volume of the vitrified HEWC, the glass loading was increased to 24 wt.% from which 21% are Al<sub>2</sub>O<sub>3</sub>. This was possible by using a glass frit without any Al<sub>2</sub>O<sub>3</sub>.

Inactive and hot vitrification runs have shown that less than 5% of the Hg in the HEWC is fixed in the waste glass. The remaining of 95% evaporates on the glass pool surface. The Hg-vapour formed condensates in the wet part of the off-gas line. Therefore most of the Hg is fixed together with the secondary waste in bitumen.

The first active vitrification campaign will be completed in September 1987. Then, a new melter will be installed and in 1988 the HEWC-vitrification will be continued.

### 4. Vitrification of HAWC-WAK

It is planned to transport the 1989 anticipated quantity of 80 m<sup>3</sup> HLLW from the WAK in Karlsruhe to Mol/Belgium and to vitrify it in the PAMELA-plant. Detailed investigations of the HAWC-transport revealed no severe transport problems.

The composition of the HAWC-WAK, shown in Fig.1, does not differ significantly from WAW-waste. It contains comparatively high amounts of Na and U.

The development of the glass frit, similar to the VG 98/12.2 (see Fig.5), has just started at KfK. Inactive vitrification tests are planned for the end of 1987 and the hot operation in the PAMELA-plant for July 1989.

#### Process chemistry of HLLW-vitrification

The LEWC-HLLW vitrified in the PAMELA-plant is quite different in composition and activity as compared with the HLLW of the Wackersdorf plant (Fig.1). The concentration of fission products in the LEWC is relatively low and consequently also the amount of the noble metals Ru, Rh, Pd. For this reason reliable predictions about the behaviour of the WAW-HLLW in the ceramic melter cannot be made. In Table 4 the noble metal contents in the different waste glasses are shown and in addition the total throughput of noble metals per year in the WAW-plant.

Larger amounts of conductive metallic particles in the glass melt may heavily interfere with the electrical fields in the glass melt causing a decrease of homogeneous dissipation of heat. Therefore a first inactive vitrification test on a technical scale has been performed in KfK to vitrify a HLLW-simulate with the full content of the noble metals Ru and Pd. The main results of this campaign were reported at the last meeting in Tokyo.

With the increasing amount of noble metals fed into the melter, the voltage and the power input decreased particularly of the electrodes near the melter bottom. At the end of the run the electrical power was lower by a factor of 4 and the temperature of the glass melt decreased.

Substantial amounts of  $\text{PdTe}_x$  and  $\text{RuO}_2$  have agglomerated at the melter floor forming a suspension of increased viscosity and high electrical conductivity. As this agglomeration could be a serious problem for the vitrification of HLLW, the distribution and chemical form of the noble metals in the waste glass and especially in the glass layer at the melter bottom have been studied.

The Ru exists in the glass melt in form of  $\text{RuO}_2$ . Pd however forms tellurides ( $\text{PdTe}_x$ ). In the produced glass block the  $\text{RuO}_2$  and  $\text{PdTe}_x$  are homogeneously dispersed in form of small particles. The diameter of the spherical Pd-tellurides are between 1 and 12  $\mu\text{m}$  with a maximum at 5  $\mu\text{m}$ . The  $\text{RuO}_2$  particles form idiomorphic crystals smaller than 1  $\mu\text{m}$ . Analysis of the glass product revealed that from the total Pd- and Ru-amount fed into the melter (about 12 kg Pd and 13.5 kg Ru) only 35% were in the out-pouring glass melt. The remaining 65% was found in the glass layer at the melter bottom after the melter has been emptied at the end of the vitrification runs. In samples, taken by core drilling from the 40 mm thick glass layer, high contents of  $\text{RuO}_2$  and  $\text{PdTe}_x$  have been found.

Cross-sections of the drill core samples are shown in Fig.3. Besides very fine particles of  $\text{RuO}_2$  there exists larger droplets of PdTe up to 5 mm forming a loose suspension of higher viscosity. Both compounds  $\text{RuO}_2$  and  $\text{PdTe}_x$  are metallic conductors and this explains the high electrical conductivity of the glass layer. The remobilization of the noble metal-rich bottom layer was successfully achieved some weeks later. The melter was filled up again with glass frit and before and during draining inert gases were bubbled through the glass melt.

The  $\text{PdTe}_x$ , with a Te-content of between 8 and 20%, are liquid down to about  $800^\circ\text{C}$  as it is known from a study of the Pd-Te-system which is currently under investigation. This explains the special morphology of the  $\text{PdTe}_x$ . The arrows in the Pd-rich part of the phase-diagram in Fig.4 mark the compositional variations observed in the agglomeration and the triangle indicates the highest temperature in the melter. In this region the  $\text{PdTe}_x$  are liquid down to  $800^\circ\text{C}$  and therefore larger droplets can be formed which sedimentate to the melter floor. The small PdTe-particles in the glass product have a lower Te-content and are therefore solid in the melting range of  $1150^\circ\text{C}$ . That explains why they do not grow into larger particles.

For longterm HLLW-vitrification runs, the agglomeration and sedimentation of the noble metals must be avoided. This could be reached by different methods

a) Chemical method

Under more oxidizing conditions the Te in the glass melt could be oxidized to  $\text{TeO}_2$ . Te-rich liquid  $\text{PdTe}_x$ -droplets could not be formed which grow and sedimentate to the melter bottom.

b) Melter design

The ceramic melter for the Wackersdorf plant will have a floor with an inclination of  $45^\circ$  to the bottom drain hole. Investigations have shown that a  $45^\circ$  inclination is necessary to remobilize a viscose glass layer at the melter bottom.

c) Gas bubbling

By bubbling inert gases through several pipes in the glass melt, agglomerations at the melter bottom can be remobilized.

Inactive experiments with noble metal containing HLLW planned in the beginning of 1988 in KfK will give us more information about the success of the different methods. In the meantime the chemical behaviour of the noble metals, their distribution and agglomeration in the glass melt is being studied by vitrification tests with a small liquid fed laboratory melter (glass melt volume about 2 l).

**Characterization of glass product GP 98/12.2  
for vitrification of WAW-HLLW**

Detailed investigations of the glass frit VG 98/12.2 and the waste glass GP 98/12.2 produced with the ceramic melter and in lab scale, for physical and chemical properties, have been performed in the past year. The composition of the glass frit is shown in Fig.5.

**1. Process parameters**

For melter operation the most important properties of the glass melt are

- viscosity
- electrical resistance

as a function of temperature.

The results of the measurements are given in Tab.5 and Tab.6. The specified viscosity value of 55 dPa·s and the resistivity of 5 cm at 1150°C are met quite well. Different waste loadings of the waste glass have no influence on viscosity and electrical resistance. An explanation for the higher viscosity of the technical waste glass has not yet been found (possibly the Na-content in the glass frit was too low).

The weight loss of the glass melt by vaporization has also been studied to estimate the effects of high temperatures on the glass during processing. The results of thermogravimetric measurement in the range of between 950°C and 1270°C are shown in Fig.6. At the melting temperature of 1150°C the weight loss is about 15 mg/cm<sup>2</sup> after 6 hours melting time.

## 2. Properties of the glass product

For final storage in a repository the most important properties of waste glasses are

- thermal stability against devitrification
- leachability.

### 2.1 Devitrification

The devitrification behaviour of the waste glass GP 98/12.2 has been studied at annealing temperatures between 650°C and 850°C and annealing times between 1 and 100 days.

X-ray diffraction analysis on glass samples annealed between 700°C and 750°C for 14 days indicated the presence of

RuO <sub>2</sub>	≤ 1	% crystallinity
PdTe <sub>x</sub>	≤ 1	% crystallinity
CaMO <sub>4</sub>	≤ 2.5	% crystallinity

After 30 days a weak crystallization of

Titanite  
[CaTiSiO<sub>5</sub>] ≤ 1 %

was observed.

The crystallization of the waste glass (growth rate, temperature of crystallization) is markedly influenced by the noble metal content. The fine insoluble noble metal particles favour the nucleation and growth of CaMoO<sub>4</sub>-crystals and shift the maximum crystallization temperature to lower temperatures. In noble metal-free glass specimens the first diffraction traces of CaMoO<sub>4</sub> are observed after 30 days at 800°C. In samples with the full content of noble metals, the first CaMoO<sub>4</sub>-reflections appear after 3 days at 700°C. The small amount of crystallization does not affect the glass properties, e.g. the leach resistance.

## 2.2 Soxhlet-leaching

Soxhlet-leach test is a very useful method to determine the durability of waste glass in comparison with other glass.

Using samples of geometrical size (10x5x5mm) from 3 different glass blocks produced in the technical vitrification runs (V103-V105) and from laboratory scale samples, leaching has been performed at 100°C for 30 days. The leaching data obtained shown in Fig.7. The normalized weight loss (g/cm<sup>2</sup>) of the lab scale samples and the glass frit is by a factor of 2 higher than the weight loss of the technical glasses. The difference could be explained by small variations in the chemical composition.

The static leach test with salt brines under repository conditions (200°C, 130 bars) was reported at the last meeting in Tokyo.

## 3. Other glass properties

As part of the product characterization program, a series of other properties was determined. These properties and results are

		glass frit VG 98/12.2	waste glass GP 98/12.2
- transformation temperature T <sub>g</sub> (°C)	=	545	542
- softening temperature T <sub>s</sub> (°C)	=	603	598
- linear coefficient of thermal expansion α (25-400°C)	=	9.5 · 10 <sup>-6</sup>	8.8 · 10 <sup>-6</sup>
- thermal conductivity for 125°C: λ (W/m°C)	=	1.10	1.10
for 300°C: λ (W/m°C)	=	1.29	1.26
- specific heat for 250°C: C <sub>p</sub> (J/g°C)	=	1.08	0.99
for 500°C: C <sub>p</sub> (J/g°C)	=	1.23	1.14
- density for RT: d (g/cm <sup>3</sup> )	=	2.577	2.768
- elasticity module for RT: E (GPa)	=	66	88

### Investigations of full-scale glass block canisters

Crack formation in HLW-glass blocks can potentially increase leaching surface area. Cracks could also reduce the heat flux in the glass block and cause as a result higher centreline temperature.

The extent of fracturing in glass blocks cooled at different rates and the effect of surface area increase on the mass loss by leaching, have been investigated in the past years. However, there is little information about the thermal stresses during cooling, their distribution and their linkage to the resulting fracturing in the glass block.

As a first step the finite element method was used to calculate the centreline temperatures during cooling of canisters. Figure 8 shows the correspondence between calculated and measured temperature graphs.

The effects of different crack widths on the radial temperature profile are calculated in Fig.9. Cracks of more than 1 mm width would lead to steep temperature profiles never observed in real glass blocks.

The centreline temperature in hot glass blocks (17 Watt/l glass) compared to inactive blocks is plotted in Fig.10. In the hot block the temperature does not fall below 300°C after cooling.

The next step is to use a stress analysis model (ADINA) that predicts the thermal stress and strain distribution in glass blocks. Parameters are size, diameter and cooling rate of the canister. The aim is the development of an optimized cooling procedure to minimize crack formation.

#### **Future activities**

The following activities in the field of HLLW-vitrification are planned at the INE/KfK:

- technical vitrification runs with noble metal containing HLLW-simulate to study the behaviour of noble metals (agglomeration) in a new designed melter
- investigation of the vitrification of SBR-HAWC including dissolver residues (glass development and characterization)
- investigation of the agglomeration of the noble metals in glass melts with different Te-contents and with different oxygen partial pressure. For these studies a liquid fed labscale melter (2 l volume) has been constructed
- determination of the increase in surface area by crack formation and computer modelling of thermal stresses in glass blocks.

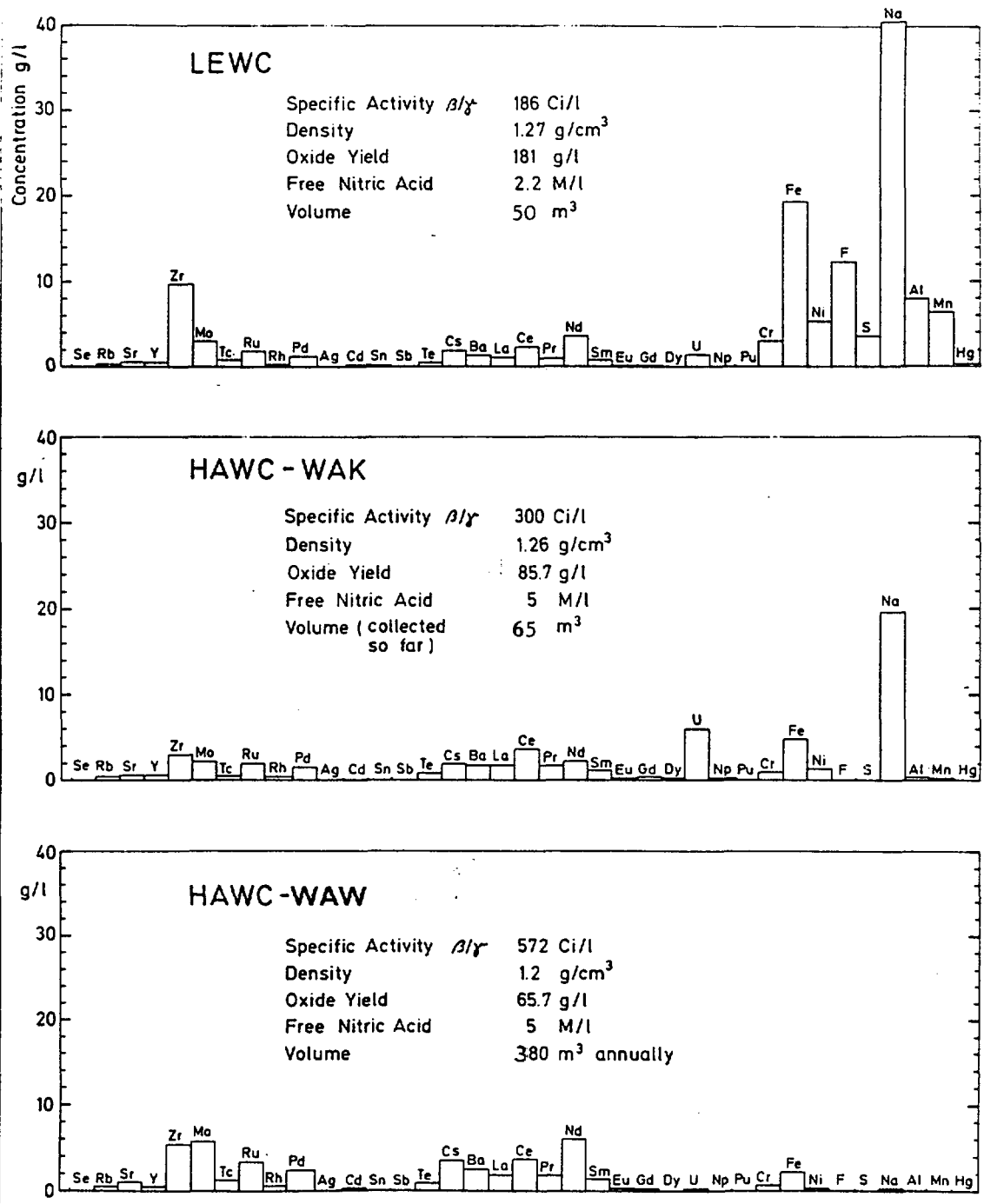


Fig.1: Comparison of element-concentrations in high-level waste solutions which are under consideration for vitrification in the FRG (the figures given for the HAWC-WAK and the HAWC-WA 350 respectively are considered to be indicative only and are of preliminary character)

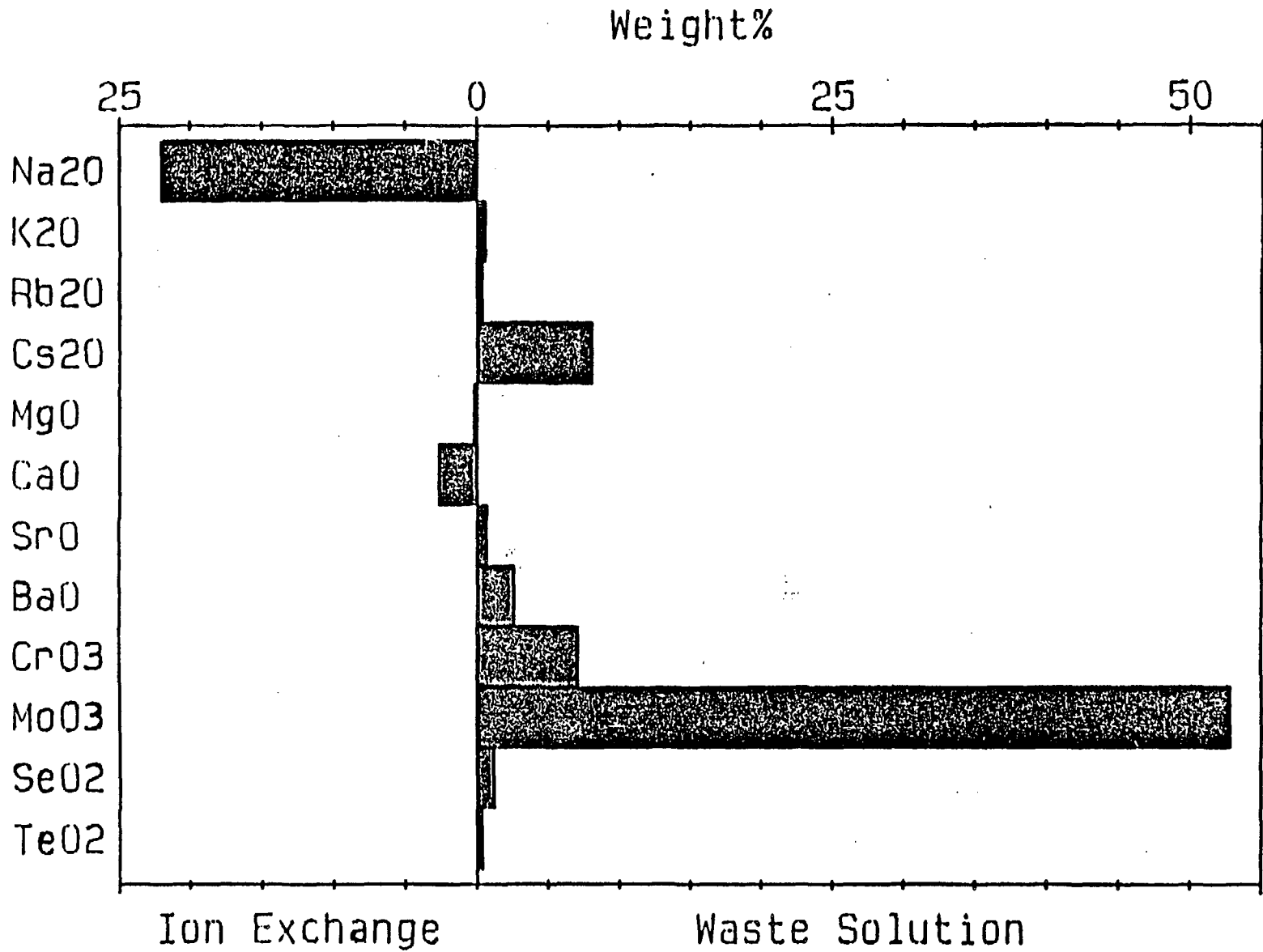
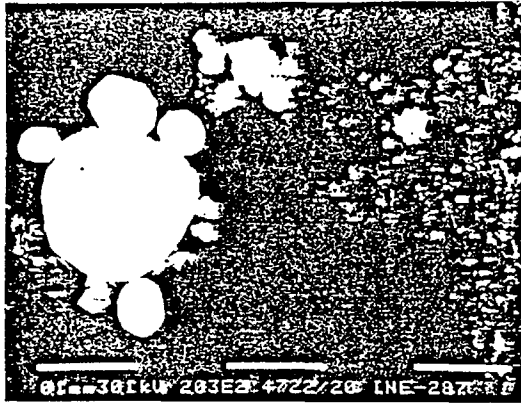
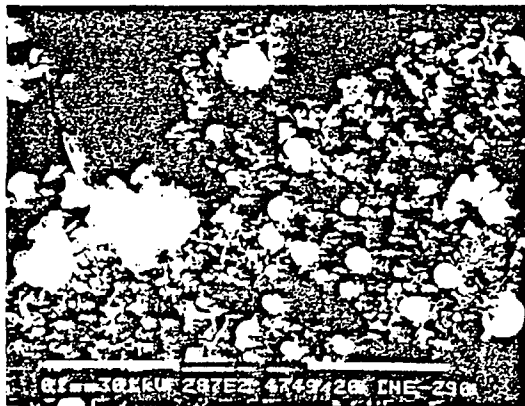


Fig. 2: Typical composition of the "yellow phase" from the HLLW vitrification process



Sample 1  
 white: PdTe<sub>x</sub>-droplets  
 grey : small particles of  
 RuO<sub>2</sub> and agglomeration  
 of RuO<sub>2</sub>



Sample 2  
 (like above)

Fig. 3: Cross sections of drill core samples taken from the glass layer at the melter bottom

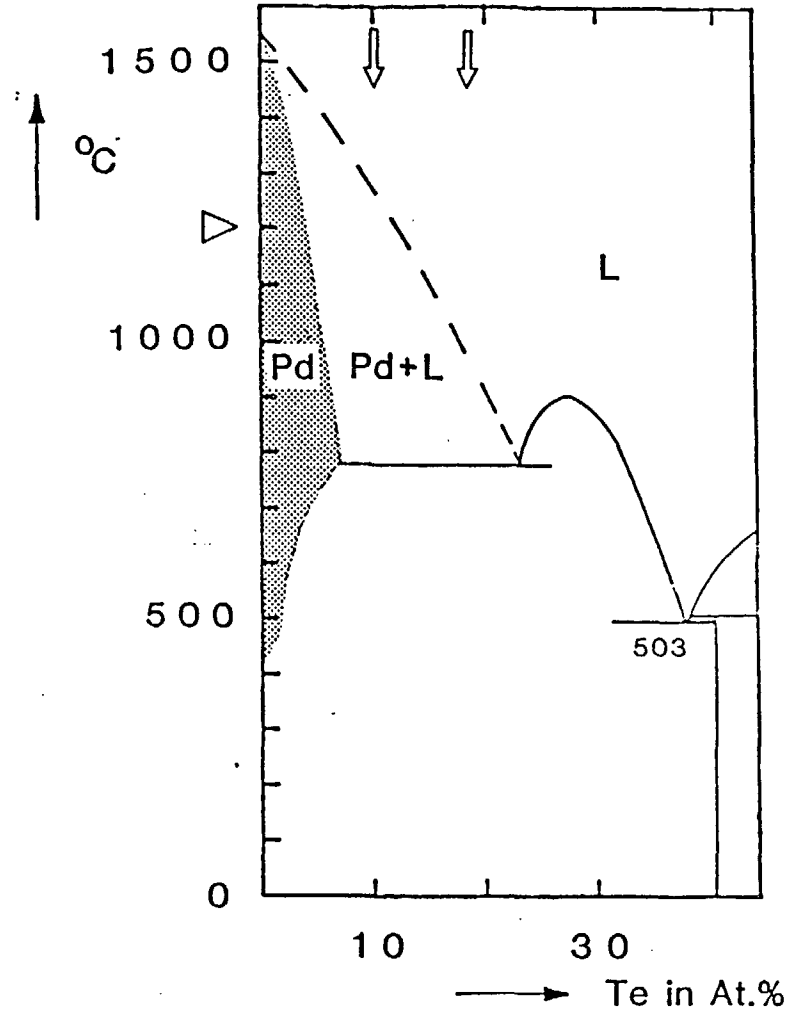


Fig. 4: Phasediagram of the Pd-rich part in the system Pd-Te

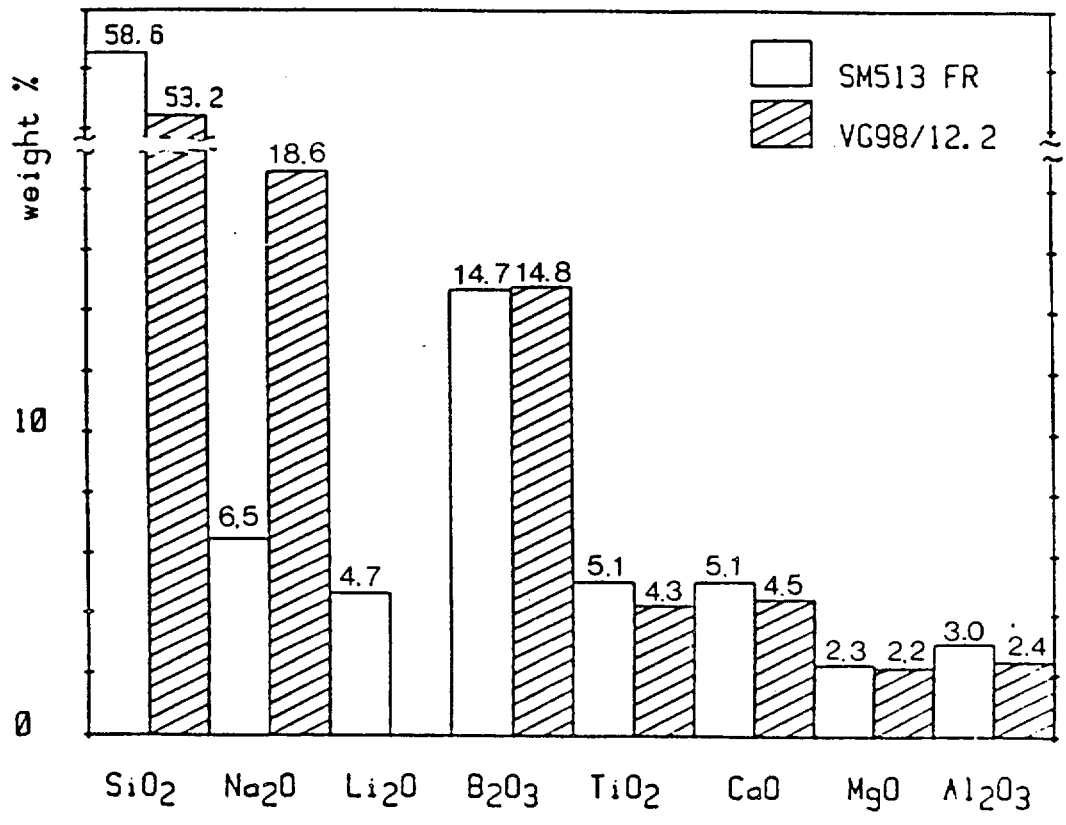


Fig. 5: Composition of the borosilicate glass frits SM 513 for PAMELA and VG 98/12.2 for HAWC-WAW

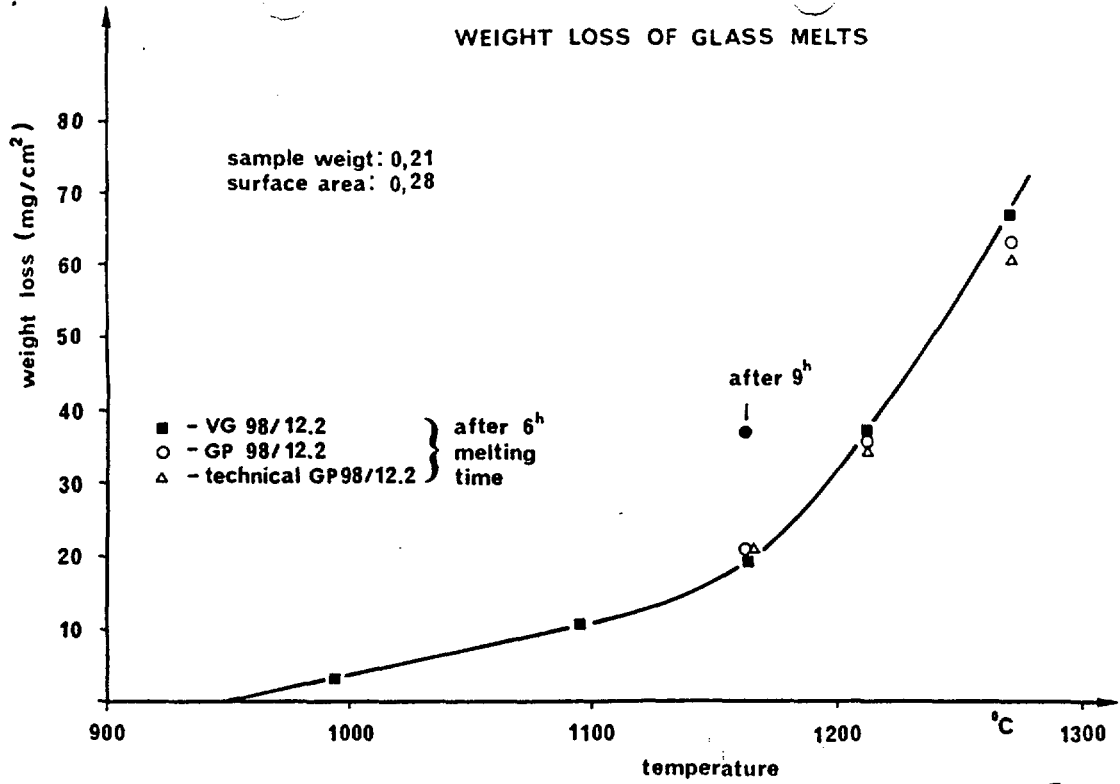


Fig. 6: Thermogravimetric measurements of the weight loss of glass melts

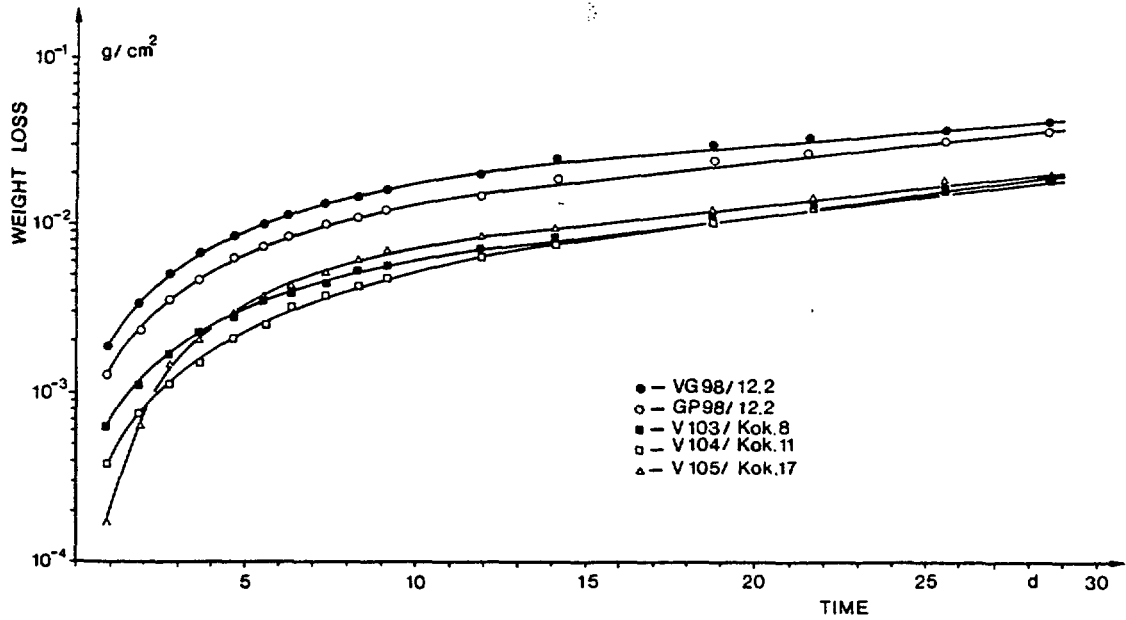


Fig. 7: Results of Soxhlet leach tests for glass frit VG 98/12.2 and labscale waste glass GP 98/12.2 as well as technical glass products (V103-V105)

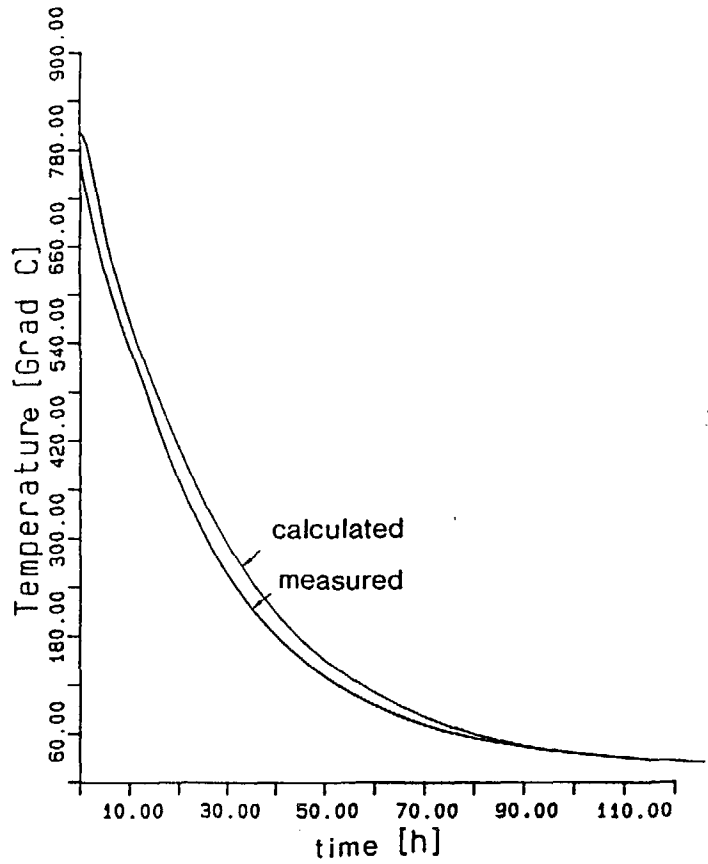


Fig. 8: Calculated and measured centrelines temperatures during cooling

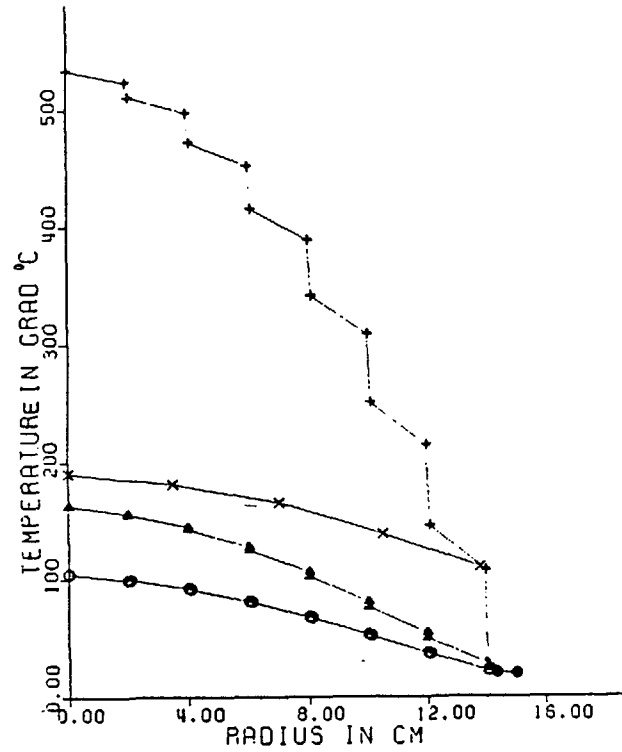


Fig. 9: Radial temperature profiles for 30 cm diameter canisters:

- x measured values
  - + 6 cracks of 1 mm width each
  - Δ 6 cracks of 0.1 mm width each
  - O without cracks
- } calculated values

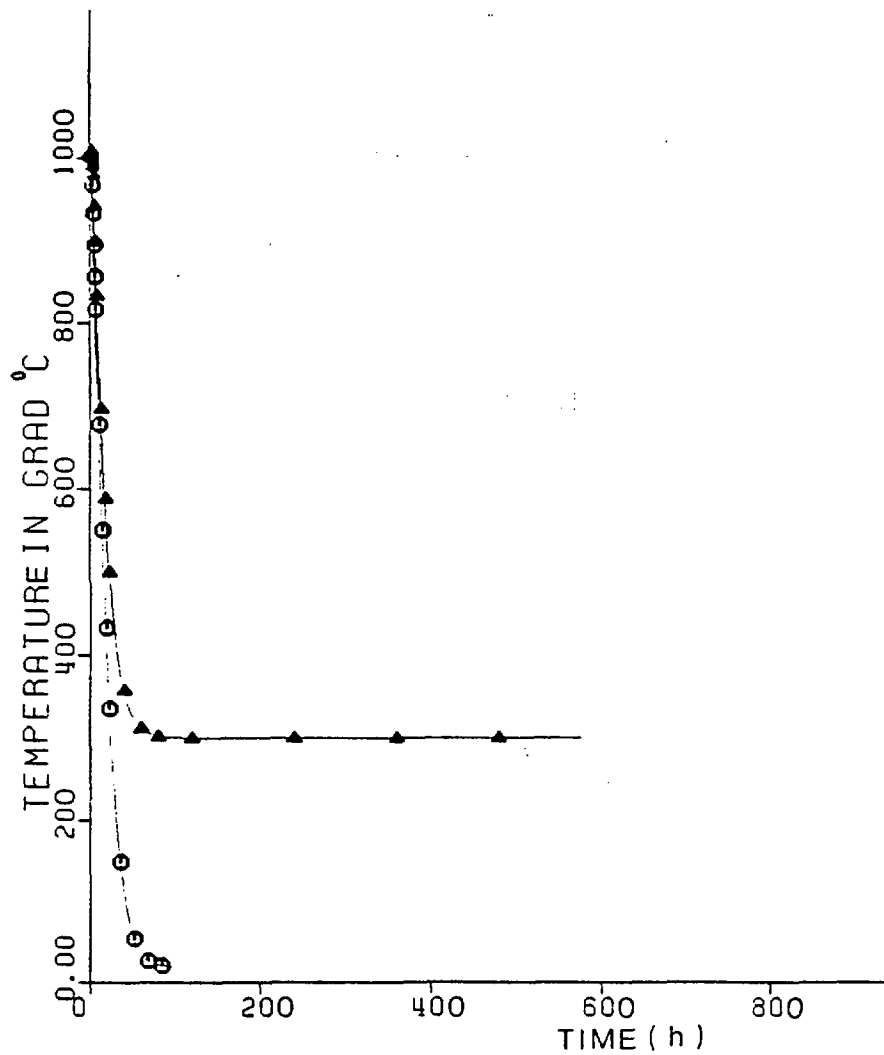


Fig. 10: Centreline temperature in a 43 cm diameter inactive and hot canister:

▲ : 17 Watt/l heat production

● : no heat production

Table I: Operation data of the LEWC-vitrification in the the PAMELA-plant

		LEWC- campaign I 10.85-12.85	LEWC- campaign II 01.86-03.86	LEWC- campaign III 04.86-05.86 (Vitromet)	LEWC- campaign IV 05.86-06.86 (rinsing)	Sum or average value cam- paign I-IV
<b>Operation times</b>						
total time of operation	(h)	1560	1461	665	744	4430
feeding time	(h)	1163	1429	610	698	3900
interruptions	(h)	397	32	55	46	530
<b>Feeding into the melter</b>						
LEWC-solution	(l)	20700	18700	5110	2700	47210
vitriified $\alpha$ -activity	(Bq)	3.16 E 14	6.70 E 14	1.82 E 14	1.16 E 14	1.28 E 15
vitriified $\beta$ -activity	(Bq)	8.65 E 16	1.24 E 17	3.28 E 16	3.50 E 16	2.78 E 17
waste oxide	(kg)	2632	3609	966	468	7675
<b>Waste glass</b>						
glass production	(kg)	30659	33396	8828	4929	77812
waste loading	(wt.-%)	8.6	10.66	10.84	9.5	9.86
glass production rate	(kg/h)	19.6	22.9	13.3	6.6	17.6
number of canisters		199	212	100	31	542
average weight of canisters (kg)		154	157.5	88.3	159	156.3/88.3
<b>Secondary waste</b>						
cold waste	(m <sup>3</sup> )	51	42.8	29	19.7	142.5
hot waste	(m <sup>3</sup> )	184	151.4	63	83	481.2
condensate	(m <sup>3</sup> )	130	126.7	58	77	39.2

## GLASS FRIT

LEWC-WASTE  
GLASS

SiO <sub>2</sub>	58.6		52.1	} 89 %
B <sub>2</sub> O <sub>3</sub>	14.7		13.1	
Al <sub>2</sub> O <sub>3</sub>	3.0		2.7	
Li <sub>2</sub> O	4.7		4.2	
Na <sub>2</sub> O	6.5		5.8	
MgO	2.3		2.0	
CaO	5.1		4.5	
TiO <sub>2</sub>	5.1		4.5	
Na <sub>2</sub> O	—	→	3.35	} 11 %
Fe <sub>2</sub> O <sub>3</sub>	—		1.69	
Al <sub>2</sub> O <sub>3</sub>	—		0.93	
ZrO <sub>2</sub>	—		0.80	
F	—		0.76	
MnO <sub>2</sub>	—		0.61	
SO <sub>3</sub>	—	→	0.54	
NiO	—		0.43	
MoO <sub>3</sub>	—	→	0.28	
Cr <sub>2</sub> O <sub>3</sub>	—		0.28	
Nd <sub>2</sub> O <sub>3</sub>	—		0.26	
CeO <sub>2</sub>	—		0.18	
RuO <sub>2</sub>	—		0.15	
Cs <sub>2</sub> O	—		0.12	
PdO	—		0.09	
Rest	—		0.53	

Tab. II: Composition of the glass frit and the LEWC-waste glass

Tab. III: Composition of calcined HEWC and major data

HEWC-Oxid	Tank 258-1		258-2		540-12	
	g/l	%	g/l	%	g/l	%
Al <sub>2</sub> O <sub>3</sub>	102.76	88.48	95.58	92.15	78.20	89.21
B <sub>2</sub> O <sub>3</sub>	0.12	0.10	0.10	0.10	0.08	0.09
CaO	0.02	0.02	0.06	0.06	0.03	0.03
CeO <sub>2</sub>	0.07	0.06	0.05	0.05	0.05	0.06
Cr <sub>2</sub> O <sub>3</sub>	0.09	0.08	0.02	0.02	0.13	0.15
Fe <sub>2</sub> O <sub>3</sub>	3.56	3.07	2.00	1.93	1.76	2.01
HgO	2.41	-	2.59	-	2.82	-
La <sub>2</sub> O <sub>3</sub>	0.04	0.03	0.03	0.03	0.03	0.03
Li <sub>2</sub> O	0.01	0.01	0.003	0.003	0.02	0.02
MgO	0.62	0.53	0.50	0.48	0.50	0.57
MnO <sub>2</sub>	0.08	0.07	0.05	0.05	0.09	0.10
MoO <sub>3</sub>	0.12	0.10	0.09	0.09	0.06	0.07
Na <sub>2</sub> O	0.62	0.53	0.29	0.28	2.45	2.80
Nd <sub>2</sub> O <sub>3</sub>	0.14	0.12	0.10	0.10	0.09	0.10
NiO	0.11	0.10	0.11	0.11	0.04	0.05
PdO	0.01	0.01	0.02	0.02	0.06	0.07
Rh <sub>2</sub> O <sub>3</sub>	0.01	0.01	0.01	0.01	0.01	0.01
RuO <sub>2</sub>	0.08	0.07	0.05	0.05	0.05	0.06
SeO <sub>3</sub>	0.17	0.15	0.15	0.15	0.12	0.14
SiO <sub>2</sub>	0.04	0.03	0.03	0.03	0.04	0.05
SO <sub>3</sub>	7.00	6.03	4.17	4.02	2.92	3.33
SrO	0.03	0.03	0.02	0.02	0.02	0.02
TaO <sub>2</sub>	0.06	0.05	0.03	0.03	0.04	0.05
TiO <sub>2</sub>	0.01	0.01	0.01	0.01	0.01	0.01
U <sub>3</sub> O <sub>2</sub>	0.06	0.05	0.02	0.02	0.01	0.01
ZrO <sub>2</sub>	0.16	0.14	0.19	0.18	0.18	0.21
F	0.15	0.13	0.04	0.04	0.67	0.76
Summe	116.14	100	103.72	100	87.66	100

Volume	173 m <sup>3</sup>	128 m <sup>3</sup>	456 m <sup>3</sup>
Waste glass loading	24 Wt%	24 Wt%	-
Activity	9.5 Ci/l	6.9 Ci/l	5.3 Ci/l

KfK

Tab. IV: Nobel metal content in the waste glass and  
nobel metal throughput in the ceramic melter

HLLW	PAMELA LEWC	WAK WAK-HAWC	Wackersdorf HAWC-WAW
Pd	0,079 %	0,280 %	0,562 %
Rh	0,022 "	0,070 "	0,131 "
RuO <sub>2</sub>	0,152 "	0,460 "	1,016 "
Waste glass loading (in t)	11 wt. % ca. 100	15 wt. % ca. 29	15 wt. % 163/a
Pd	79 kg	81 kg	916 kg/a
Rh	22 "	20 "	213 "
RuO <sub>2</sub>	152 "	133 "	1656 "

Tab. V: Viscosity of glass frit VG 98/12.2 and waste glass GP 98/12.2 produced in lab scale and in the ceramic melter

glass sample	viscosity (dPa.s)							
	temperature (°C)							
	1200	1150	1100	1050	1000	950	900	850
VG 98/12.2	34	52	89	160	323	765	2550	10100
<u>lab scale glass:</u>								
GP 98/12.2 (12,5% HAW)	38	59	103	190	390	940	3150	12750
GP 98/12.2 (15,0% HAW)	36,5	56	95	173	351	833	2750	10935
GP 98/12.2 (17,5% HAW)	34	54	97	189	412	1070	3980	18030
<u>technical glass:</u>								
campaign 103	44,5	69	121	226	470	1154	3950	16260
campaign 104	45	71	127	242	518	1314	4730	20660
campaign 105	44,5	71	129	251	548	1422	5250	23400

Tab. VI: Electrical resistance of glass frit and waste glass GP 98/12.2 produced in lab scale and in the ceramic melter

glass sample	electrical resistance ( $\Omega\text{cm}$ )								activation energy	
	temperature (°C)								Ea	
	1200	1150	1100	1050	1000	950	900	850	Kcal/Mol	
VG 98/12.2	4,5	5,4	6,4	7,7	9,5	12,8	15,1	25	13,7	
<u>lab scale glass:</u>										
GP 98/12.2 (12,5% HAW)	5,0	6,0	7,3	8,9	11,7	14,1	21,6	32	14,6	
GP 98/12.2 (15,0% HAW)	4,0	4,5	5,2	6,1	7,6	9,0	12,2	16	11,2	
GP 98/12.2 (17,5% HAW)	3,9	4,6	5,4	6,4	8,4	11,0	15,4	22	12,9	
<u>technical glass:</u>										
campaign V 103	6,2	7,4	9,0	11,3	14,8	19,7	28,0	45	15,3	
campaign V 104	5,7	6,9	8,3	10,3	12,8	18,0	25,0	38	14,7	
campaign V 105	5,6	6,7	8,2	10,3	12,7	18,0	25,0	38	15,4	